LETTERS

Transport and Anderson localization in disordered two-dimensional photonic lattices

Tal Schwartz[1], Guy Bartal[1], Shmuel Fishman[1] & Mordechai Segev[1]

One of the most interesting phenomena in solid-state physics is Anderson localization, which predicts that an electron may become immobile when placed in a disordered lattice[1]. The origin of localization is interference between multiple scatterings of the electron by random defects in the potential, altering the eigenmodes from being extended (Bloch waves) to exponentially localized[2]. As a result, the material is transformed from a conductor to an insulator. Anderson's work dates back to 1958, yet strong localization has never been observed in atomic crystals, because localization occurs only if the potential (the periodic lattice and the fluctuations superimposed on it) is time-independent. However, in atomic crystals important deviations from the Anderson model always occur, because of thermally excited phonons and electron–electron interactions. Realizing that Anderson localization is a wave phenomenon relying on interference, these concepts were extended to optics[3,4]. Indeed, both weak[5–7,31] and strong[8–11] localization effects were experimentally demonstrated, traditionally by studying the transmission properties of randomly distributed optical scatterers (typically suspensions or powders of dielectric materials). However, in these studies the potential was fully random, rather than being 'frozen' fluctuations on a periodic potential, as the Anderson model assumes. Here we report the experimental observation of Anderson localization in a perturbed periodic potential: the transverse localization of light caused by random fluctuations on a two-dimensional photonic lattice. We demonstrate how ballistic transport becomes diffusive in the presence of disorder, and that crossover to Anderson localization occurs at a higher level of disorder. Finally, we study how nonlinearities affect Anderson localization. As Anderson localization is a universal phenomenon, the ideas presented here could also be implemented in other systems (for example, matter waves), thereby making it feasible to explore experimentally long-sought fundamental concepts, and bringing up a variety of intriguing questions related to the interplay between disorder and nonlinearity.

During the past few decades, localization of light has drawn considerable attention, beginning with the suggestion that the concept of Anderson localization may be applied to electromagnetic waves[3,4]. These propositions were followed by the prediction[5] and observation[6,7,31] of coherent backscattering (weak localization). More recently, strong localization of light was observed in highly scattering dielectric media[8–11] (typically suspensions or powders of dielectric materials). These experiments demonstrated deviations from classical diffusion, signifying localization of light due to disorder. The past decade has also witnessed progress in random lasing[12], which is based on light localization in random gain media. In all of these studies, the underlying potential was fully random (no lattice), rather than 'frozen' (quenched) random fluctuations on a periodic potential, as Anderson's original model implied (see discussion in Supplementary Information).

Typical experiments studying localization of light examined transmission properties of disordered media. However, a different approach to localization of light was suggested in 1989 (ref. 13), referred to as 'transverse localization'. That concept proposed an optical system that is uniform in one ('longitudinal') direction but contains disorder in the two directions transverse to it. Such a system is described (in the paraxial limit) by a Schrödinger-like equation:

$$i\frac{\partial A}{\partial z}+\frac{1}{2k}\left(\frac{\partial^2 A}{\partial x^2}+\frac{\partial^2 A}{\partial y^2}\right)+\frac{k}{n_0}\Delta n(x,y)A=0 \qquad (1)$$

where $A(\mathbf{r})$ is the slowly-varying envelope of the time-harmonic optical field $E(\mathbf{r},t)=\mathrm{Re}[A(\mathbf{r})e^{i(kz-\omega t)}]$ of frequency ω and wavenumber $k=\omega n_0/c$, with c the vacuum light speed, n_0 and $\Delta n(x,y)$ being the average refractive index and the random fluctuations upon it, respectively. Equation (1) has no time dependence: the evolution of the light is only in space, where the propagation coordinate z replaces time in the Schrödinger equation of quantum mechanics. The localization occurs in the x–y (transverse) plane, as the diffraction-broadening of the beam is arrested by disorder[13]. Hence, the relevant wavenumber is not $k=\omega n_0/c$ but rather the transverse wavenumber, $k_\perp$, which is inversely proportional to the width of the beam, and can be much smaller (10–100 times). In our two-dimensional system, the localization length is given by[2] $\xi=l^*\exp(\pi k_\perp l^*/2)$ with $k_\perp \ll k$, where the mean free path l^* is related to the refractive-index fluctuations. We therefore recognize that even with l^* much larger than the optical wavelength $\lambda=2\pi/kn_0$, transverse localization may occur on reasonably short (experimentally accessible) propagation distances, and the fluctuations in the refractive index can be as small as 10^{-4}. Additionally, in analogy to the requirement of a time-independent potential in the corresponding quantum problem, the most stringent requirement for transverse localization is that the 'potential' $\Delta n(x,y)$ must not vary throughout propagation, otherwise Anderson localization would not occur. Thus far, there have been two pioneering attempts to observe transverse localization in arrays of optical waveguides[14,15]. However, neither has demonstrated Anderson localization, because the experiments lacked the necessary statistical aspect, and control over the disorder. Here, we demonstrate Anderson localization of light in a perturbed periodic potential: transverse localization caused by random fluctuations on a photonic lattice.

Our system (illustrated in Fig. 1a) is a two-dimensional photonic lattice with random fluctuations, represented by equation (1). The index change $\Delta n(x,y)$ contains a periodic term and fluctuations (of the same average period) superimposed on it, such that both the periodic potential and the fluctuations are z-independent. The lattice depth and the relative disorder strength are controlled independently. To make the disordered lattice, we use the optical induction technique[16], now commonly used for studying nonlinear phenomena in photonic lattices[17–23]. This technique transforms an optical

[1]Physics Department, Technion—Israel Institute of Technology, Haifa 32000, Israel.

interference pattern into a refractive-index change in a dielectric material (see Supplementary Information). Disorder is introduced by adding a speckled beam—created by passing a laser beam through a diffuser—to the interference pattern of the plane waves inducing the lattice. The disorder level is set by controlling the intensity of the speckled beam, and ranges continuously from a perfectly periodic lattice (without the speckled beam) to a strongly disordered lattice. We quantify the disorder strength by the ratio between the power of the speckled beam inducing the disorder, and the total power of the lattice-forming beams. As explained in Supplementary Information, we make the fluctuations in the lattice z-independent (propagation-invariant) by creating 'non-diffracting speckles' (a random superposition of diffraction-free Bessel beams).

After forming the disordered lattice, we launch a probe beam into it, and image the intensity distribution at the lattice output onto a CCD camera. Two representative output intensity patterns are displayed in Fig. 1. When the lattice is perfectly periodic (Fig. 1b), the probe beam undergoes 'ballistic transport', manifested by the symmetric hexagonal intensity pattern[24]. In the presence of 15% disorder (Fig. 1c), light tunnels randomly among lattice sites, producing a random intensity distribution at the lattice output after a distance L, $I(x,y,L)$. As we are dealing with a statistical problem in a finite system, it is most important to measure ensemble averages over many realizations of disorder—that is, to repeat the experiment many ($\sim$100) times under the same conditions (strength and statistics of disorder), each time with a different realization of the disorder. To do this, we vary the diffuser position, generating a new speckle pattern, which induces a new disordered lattice, with the same statistical properties as before (see Supplementary Information). The probe beam is launched into the new lattice (at the same location), and its output intensity is recorded. We test the propagation of the probe beam for 12 levels of disorder, and the statistical data for each disorder level is taken over 100 individual experiments.

Figure 2 presents the results of these statistical measurements. For each realization of disorder, the confinement of the beam at the output plane is quantified by the inverse participation ratio $P \equiv \left[\int I(x,y,L)^2 \mathrm{d}x\mathrm{d}y\right] \Big/ \left[\int I(x,y,L)\mathrm{d}x\mathrm{d}y\right]^2$, which has units of inverse area, and an average effective width $\omega_{\mathrm{eff}} = \langle P \rangle^{-1/2}$, where $\langle \cdots \rangle$ stands for averaging over multiple realizations of disorder (of the same level). Figure 2a shows the average (over 100 realizations) effective width at the lattice output as a function of disorder level, revealing that the effective width of the output probe beam decreases monotonically as the level of disorder is increased. That is, transport in the lattice is reduced by the presence of random fluctuations, even though these fluctuations are very weak ($|\Delta n|/n_0 < 2 \times 10^{-4}$). Figure 2b shows the corresponding average value of the inverse participation ratio, $\langle P \rangle$, as a function of the disorder level, along with its statistical standard deviation (marked by error bars). Figure 2b reveals that, when Anderson localization occurs, the relative fluctuations of the inverse participation ratio, $\Delta P/\langle P \rangle$, are very large—of the order of unity. This result agrees with the prediction[25,26] that the relative fluctuations in P are inversely proportional to the dimensionless diffusion coefficient ('conductance'). In our experiments, this coefficient is close to unity, so these large fluctuations are expected.

According to the scaling theory of localization, in two-dimensional systems Anderson localization always occurs, for any amount of disorder[25] (unlike three-dimensional systems, where localization occurs above some critical level of disorder). However, the localization length is exponentially large, posing a great challenge for the observation of two-dimensional localization. In the transverse localization scheme[13], a narrow beam propagating through the medium first undergoes diffusive broadening, until its width becomes comparable to the localization length. Then, localization takes place, and the beam stays localized, acquiring exponentially decaying 'tails'. As the disorder level is increased, the initial distance of diffusive propagation decreases, and the beam evolves faster into the localized

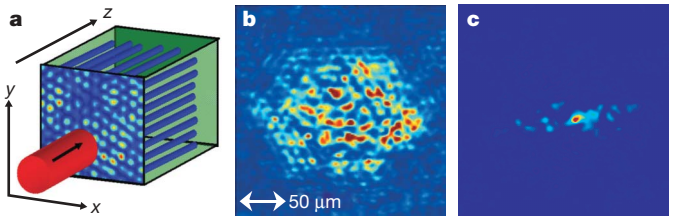

Figure 1 | Transverse localization scheme. a, A probe beam entering a disordered lattice, which is periodic in the two transverse dimensions (x and y) but invariant in the propagation direction (z). In the experiment described here, we use a triangular (hexagonal) photonic lattice with a periodicity of 11.2 μm and a refractive-index contrast of $\sim 5.3 \times 10^{-4}$. The lattice is induced optically, by transforming the interference pattern among three plane waves into a local change in the refractive index, inside a photorefractive SBN:60 ($Sr_{0.6}Ba_{0.4}Nb_2O_6$) crystal. The input probe beam is of 514 nm wavelength and 10.5 μm full-width at half-maximum (FWHM), and it is always launched at the same location, while the disorder is varied in each realization of the multiple experiments. **b**, Experimentally observed diffraction pattern after $L = 10$ mm propagation in the fully periodic hexagonal lattice. **c**, Typical experimentally observed intensity distribution after $L = 10$ mm propagation in one particular realization of the 15% disorder in the lattice.

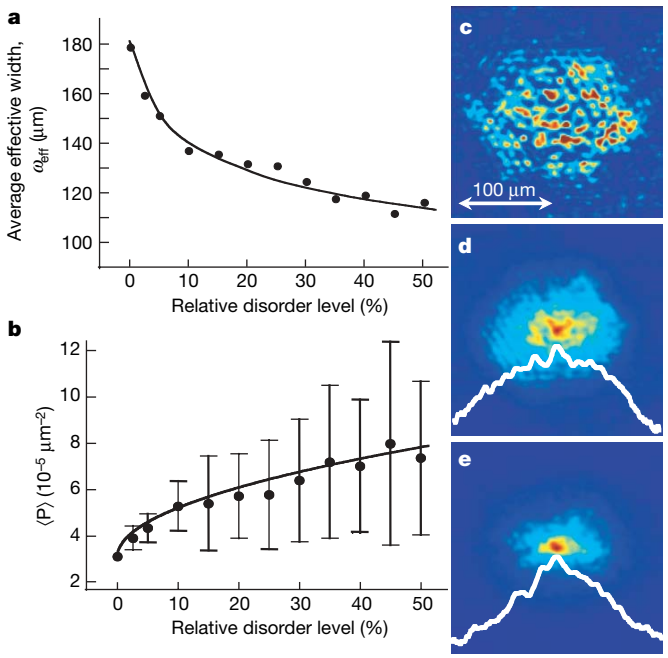

Figure 2 | Experimental results for propagation in disordered lattices. a, Ensemble-averaged effective width measured experimentally at the lattice output, as a function of disorder level. The ensemble average is taken over 100 realizations of disorder. **b**, Average inverse participation ratio as function of disorder level. The ensemble average is taken over 100 realizations of disorder. The error bars are the statistical standard deviations of P. **c**–**e**, Experimentally measured intensity distributions at the lattice output, without disorder (**c**) and with 15% (**d**) and 45% (**e**) disorder. **d** and **e** are averaged over 100 realization of disorder. The white curves show the logarithm of the averaged intensity profile, taken along the horizontal line passing through the beam's peak. In **d**, fitting the curve to a gaussian profile of the form $I \propto \exp(-2r^2/\sigma^2)$ yields the value $\sigma = 92$ μm. In **e**, the fitted curve corresponds to an intensity profile of the form $I \propto \exp(-2|r|/\xi)$, where $|r|$ is the distance from the centre of the beam, and $\xi = 64$ μm is the localization length as determined by the exponential fit. In terms of FWHM, the width of the fitted profile of **e** is 44 μm, compared to 108 μm FWHM for the gaussian fit in the diffusive case of **d**, and it is also three times narrower than the diffraction pattern observed in the absence of disorder: 120 μm (**c**). The transition from the gaussian curve of **d** to the exponentially decaying curve of **e** displays the crossover from diffusive transport (**d**) to Anderson localization (**e**).

state. Consequently, when examining the beam after a given propagation distance, the output beam should display a crossover, from diffusive transport to localization, as the disorder level is increased (to be distinguished from the localization transition, occurring in three-dimensional systems).

In order to reveal the transport properties of the disordered lattice, we average over the intensity distributions acquired at the lattice output, and examine the ensemble-average profile. Figure 2 shows $\langle I(x,y,L)\rangle$ in the absence of disorder (Fig. 2c), with moderate disorder (15%, Fig. 2d) and with strong disorder (45%, Fig. 2e). Figure 2 reveals that the (ensemble-averaged) beam intensity structure narrows as the disorder level is increased. Examining the logarithm of the intensity cross-section in Fig. 2d, taken through the peak of the ensemble-averaged intensity, reveals a gaussian shape (the parabolic curve of the logarithm, white curve in Fig. 2d), indicating diffusive broadening. This means that, for the particular level of disorder in Fig. 2d, the localization length is rather large, hence the localization effect is not observed yet. However, when the disorder is stronger (Fig. 2e), the best fit of the logarithm of the ensemble-averaged intensity profile is a linear curve, implying a structure decaying exponentially from its centre. That is, the ensemble-average intensity profile displayed in Fig. 2e exhibits Anderson localization. The transition from Fig. 2d to Fig. 2e manifests the crossover from diffusive transport to localization as the disorder level is increased.

In order to corroborate our experimental results, we simulate the propagation of the probe beam under typical experimental parameters, repeating the process with 100 different random realizations of the disorder, at each disorder level. Figure 3a shows the averaged effective width as a function of propagation distance (on a double-logarithmic scale), where each curve represents a different level of disorder, and the dashed lines designate a power-law ($\omega_{\mathrm{eff}} \propto z^{\nu}$) relation, with $\nu = 1$ and $\nu = 1/2$. For a perfectly periodic lattice, the curve approaches a constant slope with $\nu = 1$, meaning that the beam broadens linearly as it propagates in the lattice, signifying ballistic transport. When weak disorder (2.5%) is introduced, the behaviour is completely different: the curve approaches $\nu = 1/2$, indicating that the (mean) transport is now diffusive (over the range of the simulated propagation). With stronger disorder the beam first expands diffusively, but after a short propagation distance the exponent ν decreases to a value in the range $0 < \nu < 1/2$ (depending on the disorder strength), and the broadening of the beam becomes slower. At disorder levels higher than 20%, ν approaches zero, and the only change in the beam width is due to statistical fluctuations. At this stage the light is localized, and the further broadening of the beam is arrested by the disorder. This is again confirmed by calculating the logarithm of the intensity profile. As in the experimental results, in the localization regime (30% disorder, Fig. 3c), the average intensity pattern decays exponentially from the centre. In contrast to that, in the diffusive regime (2.5% disorder, Fig. 3b), the average beam has a gaussian-like profile. Following our experimental findings, corroborated by our numerical simulations, we conclude that we have indeed observed Anderson localization in disordered photonic lattices.

Finally, we study how nonlinearities affect Anderson localization. In solid-state physics, the interaction between electrons is usually considered to be an obstacle for observing Anderson localization. However, the interplay between disorder and nonlinearity may yield interesting new physical phenomena. This fundamental subject has been the subject of ongoing theoretical research[27–29], yet thus far it is not fully understood, and experimental studies are scarce[14,30]. Our system offers a convenient platform for such experiments, as nonlinearity can be added in a controlled fashion.

Figure 4a, b presents numerical results for a probe beam propagating in the disordered lattice, with focusing and defocusing Kerr-type nonlinearity. The system is described by:

$$i\frac{\partial A}{\partial z} + \frac{1}{2k}\left(\frac{\partial^2 A}{\partial x^2} + \frac{\partial^2 A}{\partial y^2}\right) + \frac{k}{n_0}\Delta n(x,y) + \sigma\frac{k}{n_0}n_2|A|^2 A = 0 \quad (2)$$

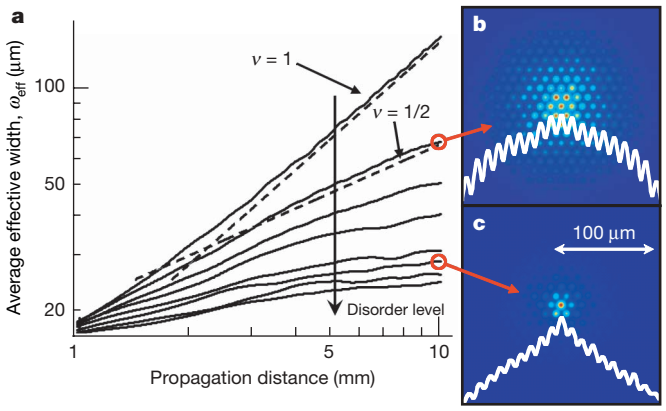

Figure 3 | Results of numerical simulations of linear propagation in disordered lattices. **a**, Averaged effective width, ω_{eff}, versus propagation distance, in a log–log plot, for different levels of disorder (0–50%). The dashed lines correspond to ballistic ($\omega_{\mathrm{eff}} \propto z$) and diffusive ($\omega_{\mathrm{eff}} \propto z^{1/2}$) transport. **b**, **c**, Averaged intensity distributions at the lattice output (after propagation of $L = 10$ mm), showing diffusive transport with a gaussian intensity profile with 2.5% disorder (**b**) and localization with an exponential decay of intensity at 30% disorder (**c**). The white curve shows the logarithm of the intensity profile, taken along the horizontal line passing through the beam's peak. The mean free path and the localization length evaluated from these simulations are approximately $l^* \approx 5$ μm and $\xi \approx 29$ μm, respectively (see calculation details in Supplementary Information).

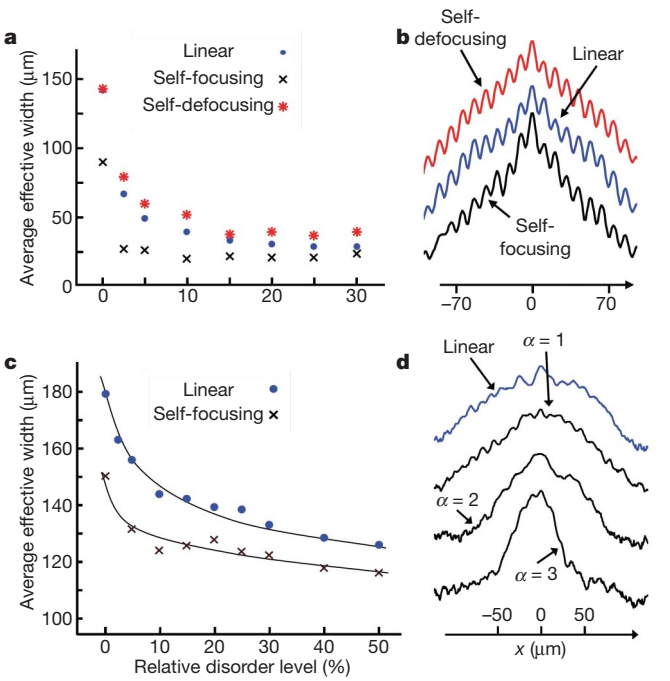

Figure 4 | Numerical (top row) and experimental (bottom row) results, showing the effects of nonlinearity on Anderson localization. **a**, Calculated effective width at the lattice output versus disorder level for linear and nonlinear propagation. **b**, Calculated intensity profiles (on a logarithmic scale) at the lattice output after linear and nonlinear propagation with 15% disorder. **c**, Experimentally measured effective width at the lattice output versus disorder level for linear propagation (upper blue curve) and under self-focusing conditions (lower black curve), for $L = 10$ mm of propagation (the lines are guides to the eye). **d**, Experimental results for the ensemble-average intensity profile (on a logarithmic scale) with 15% disorder, and increasing strengths of a focusing-type nonlinearity ($\alpha = 1$, 2 and 3, black curves), compared to linear propagation (blue curve). The ensemble average is taken over 100 different realizations of the disordered lattice, and all data are taken after $L = 10$ mm of propagation. The self-focusing nonlinearity enhances localization: the localization length decreases as the nonlinearity increases.

where n_2 scales the strength of the nonlinearity, $\sigma = 1$ ($\sigma = -1$) standing for self-focusing (self-defocusing). In Fig. 4a, the maximal nonlinear contribution $n_2|A|^2$ is 15% of the lattice depth. Figure 4a shows the output averaged effective width, for different values of disorder. In the absence of disorder, the self-focusing strength is insufficient to form a lattice soliton[17,18], yet it does reduce the diffraction broadening. The general trend of all three generic cases (linear, self-focusing and defocusing) is similar: disorder suppresses transport. In the presence of self-focusing, the initial (at low disorder levels) reduction in the width of the average output beam is much steeper than in the linear case. At high disorder levels, where localization takes place, the difference between linear and nonlinear propagation is reduced, and the behaviour is dominated primarily by disorder. In contrast, the effect of defocusing is minor at all disorder levels: the width of the average output beam is slightly increased due to self-defocusing (which acts to spread the beam faster than its linear diffraction). After a short propagation distance, in which the beam has broadened and its intensity has diminished, the remaining propagation is essentially as if the medium were linear. A more interesting behaviour is revealed in Fig. 4b, showing the logarithm of the intensity profile of the output beam, under the combined action of 15% disorder and self-focusing (lower graph), self-defocusing (top) and linear propagation (middle). For this disorder level, the localization regime, during linear propagation, is not yet reached, as the average beam profile is non-exponential. Again, the defocusing effect is minor: the average intensity profile is only slightly broader. However, under self-focusing, the beam becomes localized with exponentially decaying tails (bottom curve in Fig. 4b). This clearly indicates that self-focusing enhances localization. That is, in the presence of an 'attractive nonlinearity', localization is observed at lower levels of disorder, for a given (finite) propagation distance. We therefore study the combined effects of disorder and nonlinearity experimentally, for the particular case studied numerically in Fig. 4a.

The results are shown in Fig. 4c, where we compare the averaged effective width as a function of disorder level, for the linear case (upper curve, circles), and under self-focusing nonlinearity (lower curve, crosses), where the nonlinearity strength is set by making the probe intensity equal to the interference maxima of the lattice-writing beams (for a perfect lattice). These experiments show that self-focusing enhances localization effects. Figure 4d emphasizes this observation: shown are the ensemble-averaged intensity profiles (logarithmic scale) for a lattice with 15% disorder at various strengths of nonlinearity. We denote by α the ratio between the peak intensity of the probe beam and the maximum intensity of the lattice-forming beams, and perform statistical measurements for $\alpha = 1$, 2 and 3 (black curves in Fig. 4d). Comparing the logarithm of the averaged intensity profile to that of linear propagation (blue curve in Fig. 4d), we observe the effect predicted by the simulation: for $\alpha = 1$, self-focusing enhances localization, altering the intensity profile from diffusive-like to exponentially decaying. As the nonlinearity is made stronger, the intensity profile narrows down further ($\alpha = 2$), until, at $\alpha = 3$, the output beam profile resembles the input profile, suggesting the formation of a soliton. This kind of 'average soliton', forming in the highly nonlinear disordered lattice, is in fact an ensemble-average over many realizations of disorder, which survives the lattice imperfections. Such an 'average soliton' has not, to our knowledge, been observed before.

Our methods for real-time induction of photonic lattices with controlled disorder embedded in them, which have facilitated the observation of Anderson localization and the effects of nonlinearity on localization, offer an elegant means for its statistical exploration. We anticipate that the methods presented here will become a standard tool in future experimental research on transverse localization. They should also prove useful in future work on the influence of nonlinearity on localization, where a variety of intriguing questions arise. For example, can solitons form in the presence of random fluctuations in a nonlinear periodic structure? Can modulation instability and spontaneous pattern formation occur in perturbed nonlinear lattices? These and related questions are now accessible experimentally in our system.

Received 6 November 2006; accepted 25 January 2007.

1. Anderson, P. W. Absence of diffusion in certain random lattices. *Phys. Rev.* **109,** 1492–1505 (1958).
2. Lee, P. A. & Ramakrishnan, T. V. Disordered electronic systems. *Rev. Mod. Phys.* **57,** 287–337 (1985).
3. John, S. Electromagnetic absorption in a disordered medium near a photon mobility edge. *Phys. Rev. Lett.* **53,** 2169–2172 (1984).
4. Anderson, P. W. The question of classical localization: a theory of white paint? *Phil. Mag. B* **52,** 505–509 (1985).
5. Akkermans, E. & Maynard, R. Weak localization of waves. *J. Phys. Lett.* **46,** 1045–1053 (1985).
6. Van Albada, M. P. & Lagendijk, A. Observation of weak localization of light in a random medium. *Phys. Rev. Lett.* **55,** 2692–2695 (1985).
7. Wolf, P. E. & Maret, G. Weak localization and coherent backscattering of photons in disordered media. *Phys. Rev. Lett.* **55,** 2696–2699 (1985).
8. Wiersma, D. S., Bartolini, P., Lagendijk, A. & Righini, R. Localization of light in a disordered medium. *Nature* **390,** 671–673 (1997).
9. Berry, M. V. & Klein, S. Transparent mirrors: rays, waves and localization. *Eur. J. Phys.* **18,** 222–228 (1997).
10. Chabanov, A. A., Stoytchev, M. & Genack, A. Z. Statistical signatures of photon localization. *Nature* **404,** 850–853 (2000).
11. Störzer, M., Gross, P., Aegerter, C. M. & Maret, G. Observation of the critical regime near Anderson localization of light. *Phys. Rev. Lett.* **96,** 063904 (2006).
12. Cao, H. *et al.* Random laser action in semiconductor powder. *Phys. Rev. Lett.* **82,** 2278–2281 (1999).
13. De Raedt, H., Lagendijk, A. & de Vries, P. Transverse localization of light. *Phys. Rev. Lett.* **62,** 47–50 (1989).
14. Pertsch, T. *et al.* Nonlinearity and disorder in fiber arrays. *Phys. Rev. Lett.* **93,** 053901 (2004).
15. Eisenberg, H. *Nonlinear Effects in Waveguide Arrays*. PhD thesis (supervisor Y. Silberberg) Weizmann Institute of Science (2002).
16. Efremidis, N. K., Sears, S., Christodoulides, D. N., Fleischer, J. W. & Segev, M. Discrete solitons in photorefractive optically induced photonic lattices. *Phys. Rev. E* **66,** 046602 (2002).
17. Fleischer, J. W., Carmon, T., Segev, M., Efremidis, N. K. & Christodoulides, D. N. Observation of discrete solitons in optically induced real time waveguide arrays. *Phys. Rev. Lett.* **90,** 023902 (2003).
18. Fleischer, J. W., Segev, M., Efremidis, N. K. & Christodoulides, D. N. Observation of two-dimensional discrete solitons in optically induced nonlinear photonic lattices. *Nature* **422,** 147–150 (2003).
19. Neshev, D. N. *et al.* Observation of discrete vortex solitons in optically induced photonic lattices. *Phys. Rev. Lett.* **92,** 123903 (2004).
20. Fleischer, J. W. *et al.* Observation of vortex-ring "discrete" solitons in 2D photonic lattices. *Phys. Rev. Lett.* **92,** 123904 (2004).
21. Cohen, O. *et al.* Observation of random-phase lattice solitons. *Nature* **433,** 500–503 (2005).
22. Trompeter, H. *et al.* Bloch oscillations and Zener tunneling in two-dimensional photonic lattices. *Phys. Rev. Lett.* **96,** 053903 (2006).
23. Freedman, B. *et al.* Wave and defect dynamics in nonlinear photonic quasicrystals. *Nature* **440,** 1166–1169 (2006).
24. Bartal, G. *et al.* Brillouin zone spectroscopy of nonlinear photonic lattices. *Phys. Rev. Lett.* **94,** 163902 (2005).
25. Abrahams, E., Anderson, P. W., Licciardello, D. C. & Ramakrishnan, T. V. Scaling theory of localization: Absence of quantum diffusion in two dimensions. *Phys. Rev. Lett.* **42,** 673–676 (1979).
26. Mirlin, A. D. Statistics of energy levels and eigenfunctions in disordered systems. Phys. Rep. **326,** 259–382 (2000).
27. Devillard, P. & Souillard, B. Polynomially decaying transmission for the nonlinear Schrödinger equation in a random medium. *J. Stat. Phys.* **43,** 423–439 (1986).
28. Doucot, B. & Rammal, R. Invariant-imbedding approach to localization. II. Nonlinear random media. *J. Phys.* **48,** 527–546 (1987).
29. Li, Q., Soukoulis, C. M., Pnevmatikos, St & Economou, E. N. Scattering properties of solitons in nonlinear disordered chains. *Phys. Rev. B* **38,** 11888–11891 (1988).
30. McKenna, M. J., Stanley, R. L. & Maynard, J. D. Effects of nonlinearity on Anderson localization. *Phys. Rev. Lett.* **69,** 1807–1810 (1992).
31. Etemad, S., Thompson, R. & Andrejco, M. J. Weak localization of photons: universal fluctuations and ensemble averaging. *Phys. Rev. Lett.* **57,** 575–578 (1986).

Supplementary Information is linked to the online version of the paper at www.nature.com/nature.

Acknowledgements We are indebted to our colleagues B. Shapiro and E. Akkermans for discussions on Anderson localization. This research was supported by the Israeli Science Foundation, by the German-Israeli DIP Project, and by the Russell Berrie Nanotechnology Institute at the Technion, Israel.

Author Information Reprints and permissions information is available at www.nature.com/reprints. The authors declare no competing financial interests. Correspondence and requests for materials should be addressed to M.S. (msegev@tx.technion.ac.il).